High-Order Harmonic Generation Spectroscopy of Correlation-Driven Electron Hole Dynamics

Jonathan Leeuwenburgh,[1] Bridgette Cooper,[1] Vitali Averbukh,[1] Jonathan P. Marangos,[1] and Misha Ivanov[1,2]

[1]*Blackett Laboratory, Imperial College London, London SW7 2AZ, United Kingdom*

[2]*Max Born Institute, Max-Born-Strasse 2A, 12489 Berlin, Germany*

(Received 10 July 2013; published 20 September 2013)

We show how high-order harmonic generation spectroscopy can be used to follow correlation-driven electron hole dynamics with attosecond time resolution. The technique is applicable both to normal Auger transitions and to electron hole migration processes that do not lead to secondary electron emission. We theoretically simulate the proposed spectroscopy for $M_{4,5}NN$ Auger decay in Kr and for correlation-driven inner-valence hole dynamics in trans-butadiene and propanal.

DOI: 10.1103/PhysRevLett.111.123002 PACS numbers: 32.80.Hd, 31.50.Df, 42.65.Ky, 42.62.Fi

Time resolving ultrafast hole dynamics induced by photoionization and driven by electron correlation is among the key objectives of attosecond spectroscopy. If the energy of the formed hole state is above the double ionization threshold, it decays (typically exponentially) by the Auger mechanism [1], i.e., by emission of a secondary electron. This decay can be resolved by attosecond streaking spectroscopy whereby the Auger electron is accelerated by an IR field as it appears in the continuum [2]. Hole dynamics becomes richer if the ionized state lies below the double ionization threshold [3]. Then, the single-hole ($1h$) configuration can still decay due to strong coupling to the bound two-hole–one-particle ($2h$-$1p$) configurations [4]. Qualitatively, this decay can be understood as an Auger-type transition into bound (e.g., Rydberg) states instead of the continuum. In contrast to the Auger decay, such bound-bound transitions lead to nonmonotonic evolution of the electron density and are not accompanied by secondary electron emission [3]. Such processes cannot be resolved by attosecond streaking, and have not been observed experimentally thus far. Here we propose a technique for resolving both these and normal Auger dynamics with attosecond to femtosecond resolution.

Our technique is based on the detection of high-order harmonic generation (HHG) radiation produced by a combination of an extreme ultraviolet (XUV) pulse and an IR field. The scheme is illustrated in Fig. 1 for the case of Auger decay. The XUV core ionization occurs in the presence of the IR field, with the controlled delay between the XUV envelope and IR oscillations. The photoelectron is accelerated by the IR field and is returned by it to the parent ion, where it can recombine. Recombination results in XUV-initiated high harmonic generation (XIHHG) [5–7] and probes the presence of the hole. If the initial hole is still present, recombination brings the system back to its original state and generates *coherent* emission in the medium. If the single hole has decayed into a $2h$-$1p$ configuration (here continuum), one particle recombination into the original state is not possible and the coherent emission is suppressed. Mathematically, the intensity of the emitted light is proportional to the survival probability of the initial hole at the time recombination. The time delay between ionization and recombination is mapped onto the energy of the returning electron and, hence, on the energy of the emitted photon [8], while the hole dynamics are mapped onto the emitted harmonic intensity. The scheme is reminiscent of the probing attosecond dynamics via chirp encoded recollision (PACER) technique developed for tracking nuclear dynamics [9,10]. Unlike PACER, the reconstruction cannot benefit from isotopic substitution and relies on a completely different physical principle, as shown below. Other pertinent previous work includes HHG spectroscopy of hole dynamics in outer valence shells [11].

Realization of the proposed HHG spectroscopy requires control over the time that the XUV-ionized electron spends in the continuum before recombination (the excursion

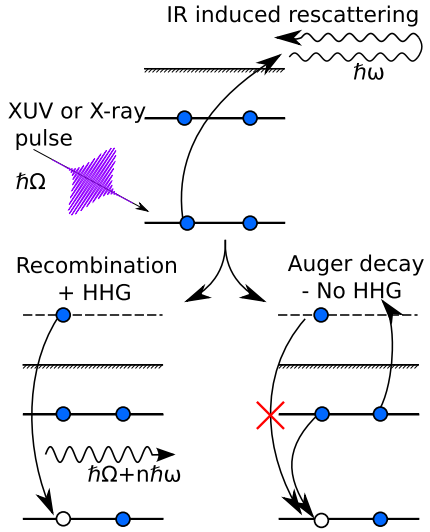

FIG. 1 (color online). Schematic of the proposed technique for the case of the normal Auger decay. The IR-driven radiative recombination and the Auger process compete for the hole formed by the XUV pulse. The longer the photoelectron spends in the continuum, the less likely it is to recombine into the initial hole and emit a high-energy photon.

time). In the example of normal Auger decay (Fig. 1), the HHG emission is suppressed exponentially as a function of the excursion time. The Auger lifetime can therefore be extracted from the measured variation in the HHG signal for a series of excursion times. Control over the excursion time is possible by changing a number of the field parameters, e.g., IR carrier frequency or intensity. The best practical implementation, we believe, is achieved by varying the temporal position of the ionizing attosecond XUV pulse within an optical cycle of the IR field. In this case, it is possible to tune the excursion time continuously while keeping the energy of the returning electron and hence the harmonic frequency approximately constant.

Figure 2 shows the energy of the returning electron as a function of the electron excursion time and the phase delay of the attosecond XUV pulse relative to the oscillations of the IR field. Positive phase delay ϕ_X corresponds to the XUV arriving after the peak of the IR oscillation. The results are obtained by classical simulation assuming that the XUV pulse is much shorter than the IR quarter cycle and limiting ionization times to the peak of the XUV. The electron trajectories are launched with a broad distribution of initial velocities at the origin and propagated classically, taking into account only the IR field. For mid-IR wavelengths with large electron excursion amplitudes, this is an adequate approximation. As in the regular HHG process, for each ϕ_X and sufficiently high energy, there are two classical electron trajectories returning with the same energy, the short and the long one. Here we focus on the cutoff region which is associated with a single trajectory, see circles in Fig. 2. The advantage of choosing the cutoff energy is that the emitted photon $\hbar\Omega \simeq 3.2U_p + I_{p,\chi}$ is well separated in energy from the emission associated with recombination to holes in the outer valence orbitals. As one can see from Fig. 2, by varying ϕ_X it is possible to change the excursion time corresponding to the cutoff harmonic within the range of about half optical cycle of the IR field. This defines the time window over which one can reconstruct the hole dynamics using the HHG spectroscopy.

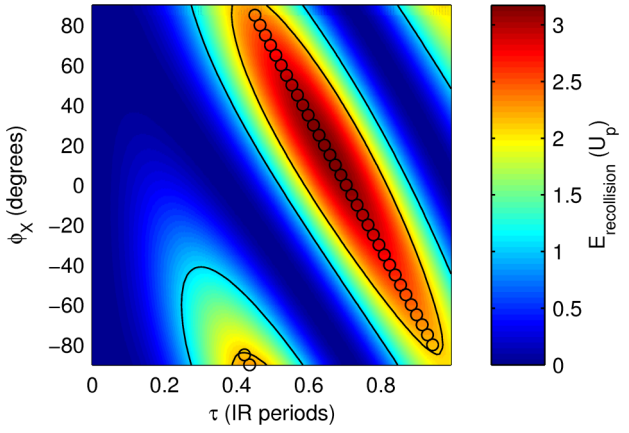

FIG. 2 (color online). Shows the classically calculated recombination energy of the electron in the units of ponderomotive potential (U_p) as a function of the position of the XUV pulse within the IR optical cycle (ϕ_X) and the classical excursion time τ. Positive ϕ_X corresponds to the XUV arriving after the peak of the IR oscillation. The full lines show contours of equal recombination energy. The circles indicate the position of the classical cut-off for each XUV position.

Mathematically, our approach can be described using the integral form of the time-dependent Schrödinger equation [12], which yields for the induced dipole (atomic units are used throughout)

$$\mathbf{D}(t) = -i\int^{t} dt' \langle g|\hat{U}_0^{\dagger}(t, t_{\mathrm{in}})\hat{\mathbf{d}}\,\hat{U}(t, t')\hat{V}_X\hat{U}_0(t', t_{\mathrm{in}})|g\rangle + \mathrm{c.c.} \tag{1}$$

Here, $\hat{V}_X$ is the interaction with the XUV pulse, $t_{\mathrm{in}} \to -\infty$ is some initial moment of time, $\hat{U}_0$ is the field-free propagator, and $\hat{U}$ is the full propagator for the system. The IR field is sufficiently weak, so that the XUV pulse dominates ionization, especially from the inner shells. On the other hand, interaction with the IR field dominates the continuum electron dynamics.

Once V_X transfers an electron to the continuum, it creates a range of ionic states. After ionization, we approximate the full propagator $\hat{U}(t, t')$ into the part that acts on the ion and the part that acts on the continuum electron, $\hat{U}(t, t') \approx \hat{U}_{\mathrm{ion}}(t, t')\hat{U}_c(t, t')$. The XUV ionization and recombination steps can be described by accurate matrix elements, but the continuum evolution between ionization and recombination is approximated by including the IR laser field but neglecting the core potential. Our approximation is similar to the quantitative rescattering theory (QRS) of strong-field ionization in IR fields [13]. Its applicability to XUV ionization in the IR field and the importance of the Coulomb-laser coupling [14] have been analyzed in Ref. [15].

Application of the continuum propagator to a state characterized by the asymptotic drift momentum $\mathbf{p}$ yields

$$\hat{U}_c(t, t')|\mathbf{p} + \mathbf{A}(\mathbf{t}')\rangle = e^{-iS(t,t',\mathbf{p})}|\mathbf{p} + \mathbf{A}(t)\rangle, \tag{2}$$

where $S(t, t') = \int_{t'}^{t} dt''[\mathbf{p} + \mathbf{A}(t'')]^2/2$ is the classical action and $\mathbf{A}(t)$ is defined as $\mathbf{F}_{\mathrm{IR}}(t) = -\partial\mathbf{A}/\partial t$. Let us denote the hole state of interest $|\chi\rangle$, characterized by the energy E_χ. The ionization potential associated with creating this hole is $I_{p,\chi} = E_\chi - E_g$, where E_g is the energy of the ground state. It is a nonstationary state, and its evolution is

$$\hat{U}_{\mathrm{ion}}(t, t')|\chi\rangle = e^{-iE_\chi(t-t')}|\chi(t - t')\rangle. \tag{3}$$

After substituting Eqs. (2) and (3) into Eq. (1) and using the saddle point method as in Ref. [16] one finds the contribution to the dipole moment associated with the creation and dynamics of hole state $|\chi\rangle$,

$$\mathbf{D}_\chi(t) = i\int^t dt' \left(\frac{2\pi}{i(t-t')}\right)^{3/2} \langle g|\hat{\mathbf{d}}|\chi(t-t'), \mathbf{p}_{\mathrm{st}} - \mathbf{A}(t)\rangle e^{-iI_{p,\chi}(t-t') - iS(t,t',\mathbf{p}_{\mathrm{st}})} F_X(t'-t_0) \times \mathbf{d}_\chi(\mathbf{p}_{\mathrm{st}} - \mathbf{A}(t')) + \text{c.c.}, \quad (4)$$

where $\mathbf{d}_\chi(\mathbf{v}) \equiv \langle \chi, \mathbf{v}|\hat{\mathbf{d}}|g\rangle$ is the ionization dipole associated with the hole state $|\chi\rangle$, and $\mathbf{p}_{\mathrm{st}}$ is the drift (canonical) momentum of the continuum electron that ensures the electron return to the parent ion, $\int_{t'}^{t}[\mathbf{p}_{\mathrm{st}} + \mathbf{A}(t'')]dt'' = 0$. The XUV pulse centered at t_0 is $F_X(t-t_0) = F_X f(t-t_0)\times \exp[-i\Omega_X(t-t_0)]$, $f(t)$ is the pulse envelope and Ω_X the carrier frequency.

We now need to evaluate the recombination dipole $\langle g|\hat{\mathbf{d}}|\chi(t-t')\rangle, \mathbf{p}_{\mathrm{st}} + \mathbf{A}(t)\rangle$. The time evolved hole state can be written as $|\chi(\tau)\rangle = a(\tau)|\chi\rangle + |\psi(\tau)\rangle$, where $\tau = t - t_0$, $a(\tau) = \langle\chi|\chi(\tau)\rangle$ is the survival amplitude of the single-hole state and $|\psi(\tau)\rangle$ is orthogonal to $|\chi\rangle$ and represents all other possible configurations. When these are dominated by continuum $2h$-$1p$ configurations (in the case of the Auger decay), or by bound $2h$-$1p$ configurations (as in the case of molecular orbital breakdown), the single-particle recombination matrix element $\langle g|\hat{\mathbf{d}}|\psi(t), \mathbf{v}\rangle$ is approximately zero. Thus, the coherent emission to the original core-hole state is described by the dipole

$$\mathbf{D}_\chi(t) \approx i\int^t dt' a(t-t')\mathbf{d}^*_\chi(\mathbf{v}_{\mathrm{st}}(t))\mathbf{d}_\chi(\mathbf{v}_{\mathrm{st}}(t')) \times \left(\frac{2\pi}{i(t-t')}\right)^{3/2} e^{-iI_{p,\chi}(t-t') - iS(p_{st},t,t')} \times F_X(t'-t_0) + \text{c.c.}, \quad (5)$$

where $\mathbf{v}_{\mathrm{st}}(t) = \mathbf{p}_{\mathrm{st}} + \mathbf{A}(t)$. The Fourier transform of this expression yields $\mathbf{D}_\chi(\Omega)$ and the harmonic spectrum is given by $I(\Omega) \propto \Omega^4|\mathbf{D}_\chi(\Omega)|^2$.

Our goal is to reconstruct $|a(t-t')|^2$. First, we show a proof-of-principle demonstration, which assumes that both the photoionization and the photorecombination matrix elements are known. We approximate the matrix elements using plane-wave continuum and the Hartree-Fock orbital for the initial hole state. This approximation has no bearing on our ability to reconstruct the hole dynamics expressed by $|a(t-t')|^2$, any form of the transition dipole can be used in Eq. (5) to simulate the reconstruction process.

Since the XUV pulse is short, for each emission frequency Ω we use the time-energy mapping in Fig. 2 to relate Ω to $\tau = t - t_0$. If the matrix elements are known and the XUV pulse is well characterized, then by monitoring how the intensity of the cutoff varies with the position of the XUV pulse we can extract $a(\tau)$ by normalizing the "observed" spectrum Eq. (5) to the theoretical spectrum where $a(\tau) = 1$. In practice, this approach would require one to use a reference spectrum obtained for a system with well characterized ionization and recombination, and with the hole that has similar ionization potential but does not decay. For our example of ionization from the $3A_g$ inner valence molecular orbital of 1,3-*trans*-butadiene, with the binding energy of 29.6 eV, such experimental reference could be the $3s$ hole in argon with binding energy of 29.2 eV.

Let us first apply our method to the exponential dynamics of the $M_{4,5}NN$ Auger decay in Kr. Its lifetime has been measured both by attosecond streaking [2] and Auger electron spectroscopy[17] and is 7.48 ± 0.35 fs. We first perform the reconstruction assuming a 2700 nm IR field and an XUV pulse with a carrier frequency of $\Omega_{\mathrm{XUV}} =$ 93 eV and a FWHM of 108 as. We then repeat the reconstruction assuming a 1300 nm IR field and an XUV pulse with a FWHM of 250 as. Changing the IR field allows us to change the window of reconstruction. In both cases we assume an intensity of 5×10^{13} W/cm^2. Results of reconstructing the Auger dynamics from the spectrum obtained using Eq. (5), normalized to the theoretical reference spectrum, are shown in Fig. 3. The reconstructed survival probability curve is in good agreement with the true one, giving the $M_{4,5}NN$ lifetime of 7.50 fs for the values obtained with 2700 nm IR, i.e., within 1% of the used value. Encouraged by this test application, we further simulate HHG spectroscopic reconstruction of the more complicated dynamics induced by molecular orbital breakdown in *trans*-butadiene and propanal.

The survival probabilities of the $3A_g$ inner valence hole in *trans*-butadiene and the $6A'$ inner valence hole in propanal were obtained using the extended second-order algebraic diagrammatic construction [ADC(2)x] method [18] within the single channel sudden approximation [19]. The single-electron Gaussian basis set [20,21] was chosen as a correlation-consistent polarized triple-zeta basis set with $3s3p$ diffuse functions for *trans*-butadiene and as a correlation-consistent polarized double-zeta basis set with $2s2p$ diffuse functions in propanal [22].

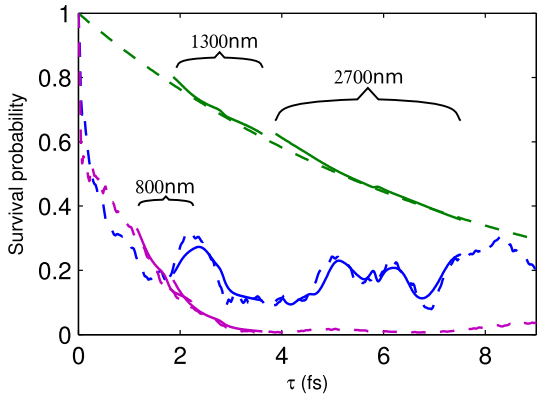

FIG. 3 (color online). Shows true (dashed lines) and reconstructed (solid lines) survival probabilities for Auger decay in krypton (upper pair of curves, green) and molecular orbital breakdown dynamics in *trans*-butadiene (middle pair of curves, blue) and in propanal (lower pair of curves, purple). Different features of decay occur at different times, different IR wavelengths are therefore used to change the window of reconstruction.

For *trans*-butadiene we use the same XUV and IR field parameters as above but with Ω_{XUV} tuned to the relevant ionization potential. Concentrating on the first and second partial revivals, we obtain an excellent agreement between original and reconstructed decay in *trans*-butadiene.

In propanal, we seek to obtain the quasiexponential decay that occurs within the first 4 fs. We use a 1300 nm IR frequency with intensity 5×10^{13} W/cm^2, and 800 nm IR at an intensity of 8.13×10^{13} W/cm^2. For both wavelengths we use a 250 as XUV FWHM pulse. We achieve excellent reconstruction of the quasiexponential decay for both IR frequencies.

The above reconstruction requires significant additional input in the form of the transition dipoles and XUV pulse shape. However, if those are not known, we can take further advantage of the short duration of the attosecond XUV pulse to rewrite Eq. (5) as

$$\mathbf{D}_\chi(t) \approx a(t-t_0) i \mathbf{d}^*_\chi(\mathbf{v}_{\mathrm{st}}(t)) \mathbf{d}_\chi(\mathbf{v}_{\mathrm{st}}(t_0)) K_\chi(t, t_0) + \mathrm{c.c.}, \quad (6)$$

where we have approximated that $a(t-t') \approx a(t-t_0)$ and that the stationary momenta in the transition matrix elements result from ionization at $t = t_0$. Here, $K_\chi(t, t_0)$ is the integral over the XUV pulse, semiclassical action, and the wave packet spreading. This integral is accumulated during the short XUV pulse and corresponds to the XUV spectral component at the frequency $\hbar\Omega_{\mathrm{st}} = I_{p,\chi} + \mathbf{v}^2_{\mathrm{st}}(t)/2$. As we change the XUV-IR phase delay $\phi_X = \omega t_0$, the initial electron velocity leading to the maximum return energy changes sign as ϕ_X crosses $\phi_0 \simeq 17.9°$. Crucially, there are values of ϕ_X on the two opposite sides of ϕ_0 that yield almost the same cutoff frequency (see Fig. 2) for the same initial electron energy, except that in the two cases the electron trajectories start in opposite directions. In a medium without preferential orientation, the product of the corresponding ionization and recombination matrix elements does not depend on the direction of the initial velocity. Thus, if we compare the cutoff intensities for the two values of ϕ_X corresponding to the same initial and almost the same final electron energies, the transition matrix elements and the terms describing the XUV pulse in Eq. (6) will approximately cancel:

$$R(\phi_X, \phi'_X) \equiv \left| \frac{a[\tau_{\mathrm{co}}(\phi_X)]}{a[\tau_{\mathrm{co}}(\phi'_X)]} \right|^2 \approx \left| \frac{D_\chi(\Omega_{\mathrm{co}}) K_\chi(\Omega_{\mathrm{co}'})}{D_\chi(\Omega_{\mathrm{co}'}) K_\chi(\Omega_{\mathrm{co}})} \right|^2. \quad (7)$$

Here, $\mathbf{v}_{\mathrm{st,co}}(t_0) = -\mathbf{v}_{\mathrm{st,co}'}(t_{0'})$ and the co subscript indicates that we consider the cutoff harmonic. Using this equation, we can now retrieve the relative decay, $R(\phi_X, \phi'_X)$ without any knowledge of the dipole transition matrix elements as D_χ is our observed spectrum and K_χ relies solely on knowledge of the XUV pulse. The results for Kr $M_{4,5}NN$ decay, $3A_g$ hole dynamics in *trans*-butadiene and $6A'$ hole dynamics in propanal are shown in Fig. 4 for

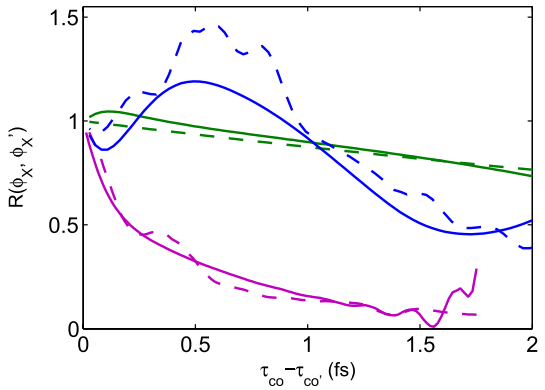

FIG. 4 (color online). Shows the true (dashed lines) and reconstructed (solid lines) relative survival probabilities resulting from the comparison of two spectra according to Eq. (7). Auger decay in krypton (upper, monotonic, green) and molecular orbital breakdown in *trans*-butadiene (upper, nonmonotonic, blue) and in propanal (lower, purple) are shown. Reconstruction of each system is performed using the largest IR wavelength shown in Fig. 3.

$\phi_X < \phi_0 < \phi'_X$. Both ϕ_X and ϕ'_X move away from or towards ϕ_0 in unison. This results in a changing $\tau_{\mathrm{co}}(\phi_X) - \tau_{\mathrm{co}}(\phi'_X)$ against which the relative survival probabilities are plotted. While the reconstruction is now not as accurate, it is still quantitative within the time window for which the approximate symmetry with respect to ϕ_0 holds. One is clearly able to distinguish between the exponential and the nonmonotonic decay (Fig. 4) and, assuming purely exponential decay, extract an Auger lifetime for krypton of 7.73 fs.

We have proposed and simulated a versatile technique for probing the correlation driven attosecond dynamics of electron holes in singly ionized atoms and molecules. This new technique does not rely on observing electrons escaping from the potential and is equally applicable to both processes which lead to secondary electron emission (e.g., Auger decay) and to those which do not (e.g., hole migration). It relies on the time-energy mapping inherent to the HHG process and allows one to deduce the hole dynamics from a series of XUV-initiated HHG spectra. Depending on the reconstruction scheme, one does or does not require knowledge of the dipole transition matrix elements to recover the hole dynamics. We illustrated our idea by changing the XUV pulse position within the IR optical cycle. The proposed HHG spectroscopy can be used for dynamical studies of a wide range of Auger and hole migration processes.

Fruitful discussions with Olga Smirnova are gratefully acknowledged. J. L. and V. A. acknowledge the financial support of the Engineering and Physical Sciences Research Council (EPSRC, UK) through the Career Acceleration Fellowship (Award No. EP/H003657/1). M. I., B. C., J. P. M., and V. A. acknowledge the financial support of the EPSRC through the Programme Grant on Attosecond

Dynamics (Award No. EP/I032517). M. I. and V. A. acknowledge the support of CORINF, a Marie Curie ITN of the European Union, Grant Agreement No. 264951. J. P. M. acknowledges the support of ERC Advanced Grant ASTEX Project No. 290467.

[1] B. Crasemann, *Atomic Inner-Shell Processes: Ionization and Transition Probabilities*, Atomic Inner-Shell Processes (Academic, New York, 1975).
[2] M. Drescher, M. Hentschel, R. Kienberger, M. Uiberacker, V. Yakovlev, A. Scrinzi, T. Westerwalbesloh, U. Kleineberg, U. Heinzmann, and F. Krausz, Nature (London) **419**, 803 (2002).
[3] V. Averbukh, U. Saalmann, and J. M. Rost, Phys. Rev. Lett. **104**, 233002 (2010).
[4] L. Cederbaum, W. Domcke, J. Schirmer, and W. von Niessen, Adv. Chem. Phys. **65**, 115 (1986).
[5] M. B. Gaarde, K. J. Schafer, A. Heinrich, J. Biegert, and U. Keller, Phys. Rev. A **72**, 013411 (2005).
[6] J. Biegert, A. Heinrich, C. Hauri, W. Kornelis, P. Schlup, M. Anscombe, K. Schafer, M. Gaarde, and U. Keller, Laser Phys. **15**, 899 (2005).
[7] G. Gademann, F. Kelkensberg, W. K. Siu, P. Johnsson, M. B. Gaarde, K. J. Schafer, and M. J. J. Vrakking, New J. Phys. **13**, 033002 (2011).
[8] Y. Mairesse, A. de Bohan, L. J. Frasinski, H. Merdji, L. C. Dinu, P. Monchicourt, P. Breger, M. Kovačev, R. Taïeb, B. Carr, H. G. Muller, P. Agostini, and P. Salières, Science **302**, 1540 (2003).
[9] S. Baker, J. S. Robinson, C. A. Haworth, H. Teng, R. A. Smith, C. C. Chiril, M. Lein, J. W. G. Tisch, and J. P. Marangos, Science **312**, 424 (2006).
[10] M. Lein, Phys. Rev. Lett. **94**, 053004 (2005).
[11] O. Smirnova, Y. Mairesse, S. Patchkovskii, N. Dudovich, D. Villeneuve, P. Corkum, and M. Y. Ivanov, Nature (London) **460**, 972 (2009).
[12] A. Becker and F. H. M. Faisal, J. Phys. B **38**, R1 (2005).
[13] Z. Chen, A.-T. Le, T. Morishita, and C. D. Lin, Phys. Rev. A **79**, 033409 (2009).
[14] O. Smirnova, A. S. Mouritzen, S. Patchkovskii, and M. Y. Ivanov, J. Phys. B **40**, F197 (2007).
[15] O. Smirnova, M. Spanner, and M. Y. Ivanov, J. Phys. B **39**, S323 (2006).
[16] M. Lewenstein, P. Balcou, M. Y. Ivanov, A. L'Huillier, and P. B. Corkum, Phys. Rev. A **49**, 2117 (1994).
[17] M. Jurvansuu, A. Kivimäki, and S. Aksela, Phys. Rev. A **64**, 012502 (2001).
[18] A. B. Trofimov and J. Schirmer, J. Chem. Phys. **123**, 144115 (2005).
[19] T. Åberg, Phys. Rev. **156**, 35 (1967).
[20] K. L. Schuchardt, B. T. Didier, T. Elsethagen, L. Sun, V. Gurumoorthi, J. Chase, J. Li, and T. L. Windus, J. Chem. Inform. Model. **47**, 1045 (2007).
[21] D. Feller, J. Comput. Chem. **17**, 1571 (1996).
[22] K. Kaufmann, W. Baumeister, and M. Jungen, J. Phys. B **22**, 2223 (1989).